PHYSICAL REVIEW B **80**, 041401(R) (2009)

Growth mechanism for epitaxial graphene on vicinal 6*H*-SiC(0001) surfaces: A scanning tunneling microscopy study

M. Hupalo,[1] E. H. Conrad,[2] and M. C. Tringides[1]
[1]*Department of Physics and Astronomy, Ames Laboratory, U.S. DOE, Iowa Sate University, Ames, Iowa 50011, USA*
[2]*School of Physics Georgia Institute of Technology, Atlanta, Georgia 30332, USA*
(Received 10 June 2009; published 7 July 2009)

The inability to grow large well-ordered ultra high vacuum (UHV) graphene with a specific number of layers on SiC(0001) is well known. The growth involves several competing processes (Si desorption, carbon diffusion, island nucleation, etc.) and because of the high temperatures, it has not been possible to identify the growth mechanism. Using scanning tunneling microscopy and a vicinal 6H-SiC(0001) sample, we determine that the Si desorption from steps is the main controlling process. Adjacent steps retract with different speeds and the released carbon produces large areas of bilayer graphene with characteristic "fingers" emanating from steps. If faster heating rates are used, the different Si desorption rates are avoided and single-layer graphene films extending over many microns are produced.

DOI: 10.1103/PhysRevB.80.041401 PACS number(s): 68.55.−a, 62.23.Kn, 68.35.−p, 68.37.Ef

The understanding of the structural and electronic properties of epitaxial graphene grown on SiC has proceeded rapidly since the suggestion that this material is a viable candidate for postcomplementary metal-oxide semiconductor electronics.[1–3] Graphene grown on either of the two polar faces of hexagonal SiC, the SiC(0001) silicon-terminated surface (Si face) and the SiC $(000\bar{1})$ carbon-terminated surface (C face), shows that these films behave like isolated graphene sheets.[2,4–6] While Si-face graphene films are more easily grown in UHV, the quality of these films has never achieved device levels.[3] Typically, graphene grown in UHV on the Si face is hampered by a high degree of SiC substrate roughening that leads to SiC terraces that are less than 50 nm across.[3,7–9] On the other hand, these films have a number of important advantages over C-face films. First, Si-face graphene is epitaxial with $(6\sqrt{3}\times 6\sqrt{3})$R30 periodicity[10,11] and, second, the growth is relatively slow compared to the C face[3] and tends to be approximately 1–5 layers thick. However, substantial improvement in the lateral order and domain sizes is necessary.

In this Rapid Communication, we present scanning tunneling microscopy (STM) data showing the kinetic processes that lead to bilayer (G2) and single-layer (G1) graphene growth under UHV conditions on the Si-terminated 6H-SiC(0001). We show that when the sample is heated in several steps (of $\sim$30 s at 1200 °C starting from room temperature), adjacent single steps have different evaporation rates. The initial surface vicinality is 0.005rad and the sample is not pretreated in a hydrogen atmosphere within a furnace. In this process, G2 films form which extend over SiC terraces that are least 150 nm wide. The increase in the terrace by factor of 3 (with only two layers) presents a vast optimization when both the lateral and vertical qualities of the layer are considered.[12] To avoid the formation of G2 layers, faster one-step heating rates were used (within 2 to 3 s to reach 1200 °C) that result in large G1 domains. These experiments reveal that an initial surface containing only single SiC bilayer steps is a great advantage since they allow finer control of the Si evaporation rate and therefore finer control of graphene nucleation and growth.

The substrates used in these experiments were 6H-SiC(0001) purchased from Cree, Inc.[13] The samples were graphitized in UHV ($P\sim 1\times 10^{-10}$ torr) by a direct current heating of the sample to $\sim$1200C measured with an optical pyrometer. As seen in STM images, the initial ungraphitized SiC substrate has a regular series of SiC bilayer steps (0.25 nm high) with an average terrace length $w=50$ nm. Note that H_2 etching (the common precleaning method used in epitaxial graphene growth[3]) leaves a surface with predominately three-bilayer and six-bilayer steps.[3] while in the current study single bilayer steps allow finer kinetics control.

In order to follow the graphitization process, regions of different graphene thickness must be identified. This is done using both contrast changes in the $(6\sqrt{3}\times 6\sqrt{3})$R30 modulation intensity associated with single and double graphene layers[8] and with relative step heights changes between different regions. This is demonstrated in Fig. 1 where a graphitized sample shows a number of different surface heights. The bilayer imaged in the lower panel of Fig. 1 shows a

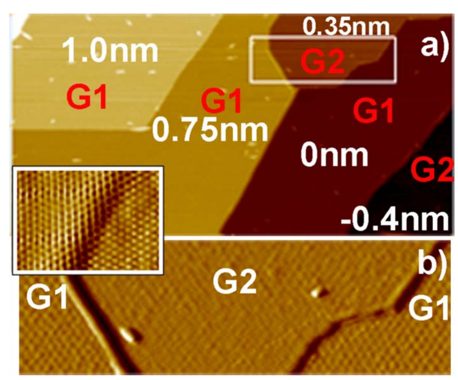

FIG. 1. (Color online) (a) 250×125 mm^2 area STM image showing different heights on a graphitized 6H-SiC(0001) sample. (b) The outlined white box of Fig. 1(a). All step heights can be written in terms of $s=0.25$ nm or $g=0.35$ nm. The small inset to the left shows that graphene grows over a step.

reduced modulation in G2 compared to G1 as previously demonstrated by Reidl *et al.*[8] All the step heights marked in Fig. 1 (0.25, 0.75, 0.4, and 0.33 nm) can be explained in terms of two heights: a bilayer SiC step $s=0.25$ nm and a graphene step $g=0.33$ nm. For instance, the 0.75 nm step is $3s$ and the 0.4 nm step is $3s$-g. It is important to note that the G2 layer forms between the SiC interface and G1. This is demonstrated in the small inset in Fig. 1 where the top graphene layer (G1) is shown, growing uninterrupted over a graphene step. This effect was also observed by Lauffer *et al.*[14]

The growth of the G2 layer is particularly unusual on SiC because stoichiometry requires the carbon contained in 3.14 SiC bilayers $[(2/a_{\mathrm{G}}^2)/(1/a_{\mathrm{SiC}}^2)=3:139]$ to form a single graphene sheet. This requirement makes the layer-by-layer growth complicated. Indeed, we find that the formation of G2 is accompanied by a transition from single SiC bilayer steps to double bilayer steps and ultimately to triple SiC bilayer steps with terraces approximately three times the starting terrace length w, i.e., $3w\sim 150$ nm. The change in the terrace length preserves the starting vicinality of the surface. A detailed look at this transition reveals a number of important characteristics of G2 growth. The three growth stages are shown in STM images in Figs. 2(a)–2(c). During the first stage, graphene islands form. The second stage is accompanied by graphene fingers that appear growing away from the SiC step edges. In the last stage, a transition to triple steps is complete and the island and fingers have merged. The scale of the images shown is very large (1 μm^2) and only G2 or G1 films are present. This is illustrated over smaller scales: in Fig. 2(c) as a 91×97 nm^2 white box shown in (d) and in Fig. 2(d) as a 28×46 nm^2 white box shown in (e). The film heights G1 and G2 are confirmed from the amplitude of the $6\sqrt{3}\times 6\sqrt{3}$ corrugation and from the difference in step heights 0.5 nm$=2s$ and 0.09 nm$=g$-s).

The details of the Si desorption from the steps can be understood by correlating the G2 area formed with local changes in the vicinality. The step height changes indicate that different types of single SiC bilayer steps release carbon at different rates causing them to retract at different speeds. A fast evaporating single step will catch up to a slower single step to form a double bilayer step. The double step subsequently merges with the slowest third step to form a triple bilayer step. At this point, there is enough carbon released in the retracting triple step to form a continuous G2 layer. In contrast, if all steps retracted by evaporating Si at the same rate, there would be a constant concentration of carbon atoms that would lead to a steady rate of G2 nucleation events. This scenario would produce a rough graphene layer contrary to the surface observed in Fig. 2(c).

Figure 2(a) shows that in the first stage of growth islands primarily nucleated within the first half of the terrace closest to the single-step edge (in a length $w/2\sim 25$ nm). The islands in Fig. 2(a) tend to be parallel with the step edges. This indicates that carbon diffusion is faster along steps rather than perpendicular to steps. More detailed statistics on island size and spacing find that the average island diameter $\langle D\rangle$ is 21.5 nm, while the average spacing $\langle L\rangle$ is 72nm. This implies that the average coverage in the region $w/2$ from the single-step edge is $\theta=\langle D\rangle/\langle L\rangle=0.33$ ML. This is in excellent agreement with the expected 1/3 ML coverage because it takes the carbon released $\sim$3 SiC bilayers to produce a single graphene layer.

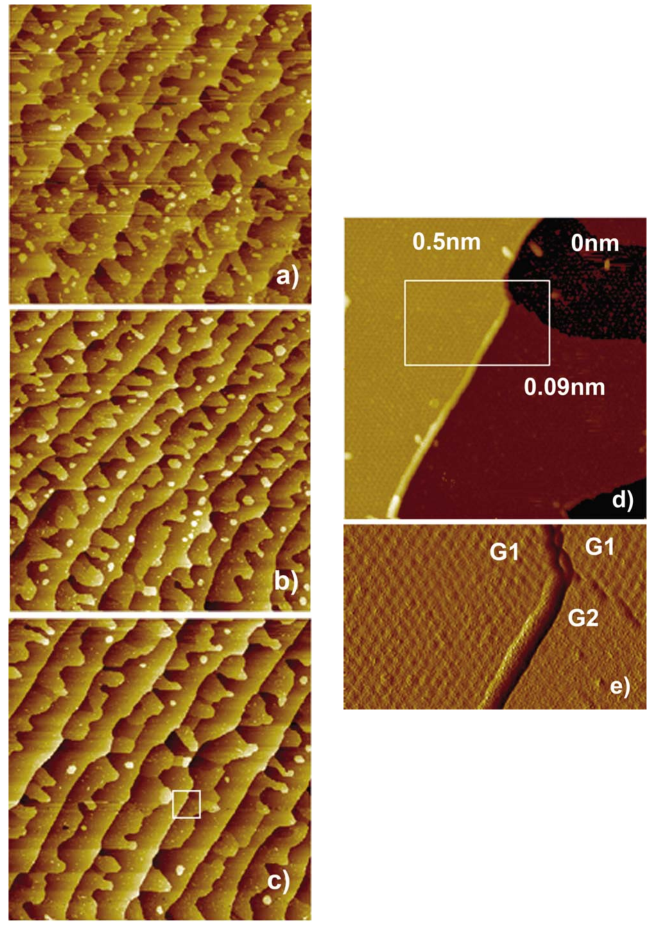

FIG. 2. (Color online) Three 1×1 μm^2 STM images of G2 graphene growth after short 30 s heating steps to 1200 °C. Three adjacent steps move with different speeds to form (a) G2 islands followed by (b) G2 fingers and finally (c) a continuous G2 layer. The 91×98 nm^2 white box outlined in (c) is shown in (d) and the 28×46 nm^2 white box in (d) is shown in (e). Both the amplitude of the corrugation and the step height difference across confirm the growth of G1 and G2 films.

The growth sequence is shown schematically in Fig. 3. Three adjacent steps evaporate Si and release carbon as they are retracting. Based on the results of Fig. 2, we infer that the

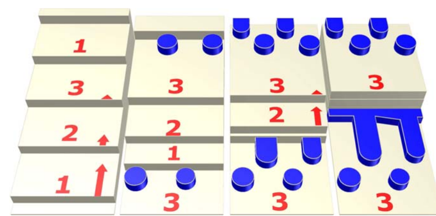

FIG. 3. (Color online) A growth model showing schematically the processes observed in Fig. 2. Three adjacent steps having different retraction speeds generate successively G2 islands, fingers, and a continuous G2 layer.

retracting speed of step 1 is larger than the retracting speed of step 2, which in turn is larger than the retracting speed of step 3. The initial G2 islands begin to nucleate in the area exposed during the retraction of the first half of the terrace associated with the fast moving step 1. Because step 1 retracts faster, it merges with step 2 to form a double SiC bilayer step. Before merging, the increased carbon released from the second half of the terrace associated with step 1 and the carbon released from step 2 combine to form fingers. Eventually, the retracting double step catches up to the slow bilayer step 3 to merge into a triple bilayer step and continuous area of G2 with smaller G1 areas remaining on the terrace.

The process outlined in Fig. 3 makes specific predictions about the areas covered by G2 at various stages of growth. These predictions can be checked against STM images. The finger coverage, when the triple step conversion is completed, is due to the carbon released from two sources. The first carbon source is the conversion of the second half of the fast step 1 terrace width ($w/2$) after islands have formed (see second panel in Fig. 3). The second carbon source comes from dissolving the two-bilayer terrace associated with step 2 of Fig. 3 (i.e, the carbon in $2w$). Because a dissolving bilayer terrace produces 1/3 of a graphene layer, the finger coverage in a terrace $3w$ long should be $(1/3)(2w+w/2)/3w=5/18$ ML=0.28. The measured finger coverage from Fig. 2(a) is 0.37 ML. The final stage (when the triple bilayer step retracts to the edge of the initial islands) requires the carbon in $3w+2w+1w$ bilayers to be converted into G2 with an area proportional to $(1/3)(3w+2w+1w)$. This amount is spread over an area proportional to $3w$, so that the G2 coverage should be $\theta=(1/3)(3w+2w+1w)/3w=2/3$ ML. The experimental value in Fig. 2(c) is found to be $\theta=0.62$ ML. Note that the initial finger diameter and finger separation are the same as the initial island diameter and island separation $D=20$ nm and $S=72$ nm, respectively. The finger separation remains unchanged as more carbon is released, but the finger width increases to $D=40$ nm. The graphene area produced along a step of length S between the time the fingers begin to form and the time the triple step transition starts is $A=1/3(w/2+2w)S=3\times10^3$ nm^2. Using this area, we can estimate the G2 finger length to be $L=A/D=75$ nm. This value is in good agreement with the 87 nm length measured in Fig. 2(b).

These experiments raise a number of interesting questions about the growth mechanism. It is known that before graphitization, a high carbon density $(6\sqrt{3}\times6\sqrt{3})$R30 surface forms.[8,15,16] X-ray measurements indicate that this layer contains $\sim2/3$ ML of carbon.[3,16] It is possible that breaking the Si-C bonds in one or two additional bilayers and the subsequent diffusion of Si through the $(6\sqrt{3}\times6\sqrt{3})$R30 interface can release the additional carbon needed to complete G1. The additional kinetic barrier of Si diffusion through G1 prohibits the easy formation of G2 and requires Si to be released from steps. Si diffusion through G1 is slower than the Si diffusion through bulk graphite because G1 is more tightly bound to the interface.[16–18]

The series of annealing cycles at low temperatures used in the experiments discussed above have identified the importance of step retraction to control Si desorption at steps. On the other hand, heating rapidly in a single heating step (2 to 3 s) with the temperature reaching 1200 °C changes the kinetics and causes G1 to nucleate faster. The surface produced by this rapid heating is shown in Figs. 4 and 13 of Ref. 3 with primarily G1 (85%). Figures 4(a) and 4(b) show a closer look at the $6\sqrt{3}\times6\sqrt{3}$R30 reconstruction in this film at two different bias voltages −0.75 V and 0.75 V, respectively. The film is identified as G1 because of the strong dependence of the $6\sqrt{3}\times6\sqrt{3}$R30 modulation on bias voltage. That is, Fig. 4(b) is more disordered than Fig. 4(a); a result previously observed by Mallet *et al.*[19] and Rutter *et al.*[20] Note the high degree of substrate order and graphene film thickness uniformity over areas larger than 2.5×2 μm^2 (see Fig. 13 of Ref. 3). While the SiC terraces are ~100 nm in Fig. 13 of Ref. 3, G1 area is significantly bigger because graphene grows over the SiC steps.[7] Because the growth of G1 is so fast, the intermediate processes (i.e., how Si is released) have not been identified.

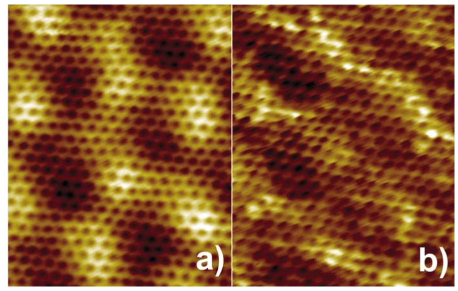

FIG. 4. (Color online) 4.33×5.5 nm^2 image at different bias voltages (a) −0.75 V 0.1 nA (left) and (b) 0.75 V 1 nA (right) showing the dependence of the $6\sqrt{3}\times6\sqrt{3}$R30 modulation on V that confirms the film is G1.

Graphene preparation is still a hotly debated problem with key controlling barriers yet to be identified. We elucidate several kinetic processes that play a crucial role in the formation of G1 and G2 on SiC: Si desorption through steps and the fine balance of different step evaporation rates and C diffusion anisotropy. Graphene domains can be grown which are an order of magnitude larger than those prepared by previous UHV methods. The most important conclusion of the current experiments is that single steps are the controlling factors for Si desorption and that different SiC steps have different evaporation rates. This result is crucial to suppress random and uncorrelated nucleation events and rougher films as in methods that rely on H_2 and start with substrates with multiple steps.[3] Although the origin of the different retraction speeds is not clear, similar differences between single-step growth rates have been observed during chemical-vapor deposition growth of SiC.[21] The temperature of Ref. 21 is higher than the one in the current study and the absolute detachment rates are different; however the relative rates and detachment barriers for each type of step have the same relation in the two experiments. These measurements reveal some of the key processes operating during graphene growth, but clearly additional theoretical work is needed to account for the different step speeds to calculate the detachment barriers and using these barriers in Monte Carlo simulations to match the observed morphologies.

We wish to thank A. Zangwill and D. Vvedensky for helpful discussions and a critical reading of the paper. Work at the Ames Laboratory was supported by the Department of Energy-Basic Sciences under Contract No. DE-AC02-07CH11358. Work at Georgia Tech was supported by a grant from the W. M. Keck Foundation and the National Science Foundation under Grants No. 0404084, No. 0521041, and No. 0820382.

[1] C. Berger, Z. Song, T. Li, X. Li, A. Y. Ogbazghi, R. Feng, Z. Dai, T. Grenet, A. N. Marchenkov, E. H. Conrad, P. N. First, and W. A. de Heer, J. Phys. Chem. B **108**, 19912 (2004).

[2] C. Berger, Z. Song, X. Li, X. Wu, N. Brown, C. Naud, D. Mayou, T. Li, J. Hass, A. N. Marchenkov, E. H. Conrad, P. N. First, and W. A. de Heer, Science **312**, 1191 (2006).

[3] J. Hass, W. A. de Heer, and E. H. Conrad, J. Phys.: Condens. Matter **20**, 323202 (2008).

[4] M. L. Sadowski, G. Martinez, M. Potemski, C. Berger, and W. A. de Heer, Phys. Rev. Lett. **97**, 266405 (2006).

[5] X. Wu, X. Li, Z. Song, C. Berger, and W. A. de Heer, Phys. Rev. Lett. **98**, 136801 (2007).

[6] W. A. de Heer, C. Berger, X. Wu, P. N. First, E. H. Conrad, X. Li, T. Li, M. Sprinkle, J. Hass, M. L. Sadowski, M. Potemski, and G. Martinez, Solid State Commun. **143**, 92 (2007).

[7] Th. Seyller, K. V. Emstev, K. Gao, F. Speck, L. Ley, A. Tadich, L. Broekman, J. D. Riley, R. C. G. Leckey, O. Rader, A. Varykhalov, and A. M. Shikin, Surf. Sci. **600**, 3906 (2006).

[8] C. Riedl, U. Starke, J. Bernhardt, M. Franke, and K. Heinz, Phys. Rev. B **76**, 245406 (2007).

[9] J. Hass, R. Feng, T. Li, X. Li, Z. Song, W. A. de Heer, P. N. First, E. H. Conrad, C. A. Jeffrey, and C. Berger, Appl. Phys. Lett. **89**, 143106 (2006).

[10] A. J. Van Bommel, J. E. Crombeen, and A. Van Tooren, Surf. Sci. **48**, 463 (1975).

[11] I. Forbeaux, J.-M. Themlin, and J.-M. Debever, Phys. Rev. B **58**, 16396 (1998).

[12] K. Emtsev, A. Bostwick, K. Horn, J. Jobst, G. Kellogg, L. Ley, J. McChesney, T. Ohta, S. Reshanov, J. Rohrl, E. Rotenberg, A. Schmid, D. Waldmann, H. Weber, and T. Seyller, Nature Mater. **8**, 203 (2009).

[13] Cree Inc., 4600 Silicon Drive, Durham, NC 27703.

[14] P. Lauffer, K. V. Emtsev, R. Graupner, Th. Seyller, L. Ley, S. A. Reshanov, and H. B. Weber, Phys. Rev. B **77**, 155426 (2008).

[15] L. I. Johansson, F. Owman, and P. Mårtensson, Phys. Rev. B **53**, 13793 (1996).

[16] J. Hass, J. Millan-Otoya, P. First, and E. Conrad, Phys. Rev. B **78**, 205424 (2008).

[17] F. Varchon, R. Feng, J. Hass, X. Li, B. N. Nguyen, C. Naud, P. Mallet, J.-Y. Veuillen, C. Berger, E. H. Conrad, and L. Magaud, Phys. Rev. Lett. **99**, 126805 (2007).

[18] A. Mattausch and O. Pankratov, Phys. Rev. Lett. **99**, 076802 (2007).

[19] P. Mallet, F. Varchon, C. Naud, L. Magaud, C. Berger, and J.-Y. Veuillen, Phys. Rev. B **76**, 041403(R) (2007).

[20] G. M. Rutter, N. P. Guisinger, J. N. Crain, E. A. A. Jarvis, M. D. Stiles, T. Li, P. N. First, and J. A. Stroscio, Phys. Rev. B **76**, 235416 (2007).

[21] T. Kimoto, A. Itoh, and H. Matsunami, J. Appl. Phys. **81**, 3494 (1997).